Inorganic Chemistry

Article

pubs.acs.org/IC

Pressure-Induced Transition from an Antiferromagnet to a Ferrimagnet for $Mn^{II}(TCNE)[C_4(CN)_8]_{1/2}$ (TCNE = Tetracyanoethylene)

Amber C. McConnell, Joshua D. Bell,[†] and Joel S. Miller*

Department of Chemistry, University of Utah, Salt Lake City, Utah 84112-0850, United States

Supporting Information

ABSTRACT: $Mn^{II}(TCNE)[C_4(CN)_8]_{1/2}$ (TCNE = tetracyanoethylene) exhibits a reversible pressure-induced piezomagnetic transition from a low magnetization antiferromagnetic state to a high magnetization ferrimagnetic state above 0.50 ± 0.15 kbar. In the ferrimagnetic state, the critical temperature, T_c, increases with increasing hydrostatic pressure and is ~97 K at 12.6 kbar, the magnetization increases by 3 orders of magnitude (1000-fold), and the material becomes a hard magnet with a significant remnant magnetization.

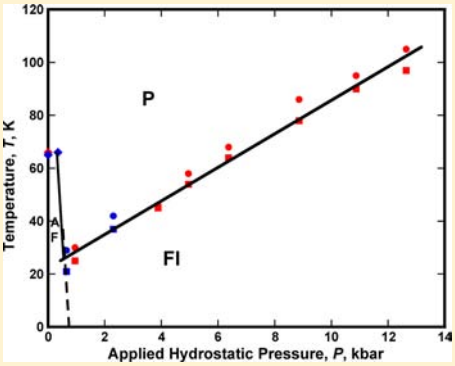

INTRODUCTION

Multifunctional materials with an integrated combination of properties are key for a myriad of future systems including transducers, sensors, and actuators. Molecular materials are particularly well suited for multifunctional materials because of their facile ability to merge properties into a single material; they exhibit a plethora of tunable properties, in part, because of the increasing availability of synthetic methodologies and strategies. Today molecule-based conductors, superconductors, magnets, and ferroics have expanded the types of substances beyond traditional solid-state materials that exhibit these properties and are poised to blend properties to develop and exploit multifunctional materials. Our results identify a molecular multifunctional material that exhibits a reversible pressure-induced piezomagnetic transition from a low magnetization antiferromagnetic state to a high magnetization ferrimagnetic state above 0.50 ± 0.15 kbar. In the ferrimagnetic state, the critical temperature, T_c, increases with increasing hydrostatic pressure and is ~97 K at 12.6 kbar, the magnetization increases by 3 orders of magnitude (1000-fold), and the material becomes a hard magnet with a significant remnant magnetization.

Since the discovery that $[Fe^{III}(C_5Me_5)_2]^{\bullet+}[TCNE]^{\bullet-}$ (TCNE = tetracyanoethylene) magnetically orders with a T_c at 4.8 K as a bulk ferromagnet,[1] other organic-based magnets having T_c values as high as 400 K (127 °C)[2,3] have been reported. These include (i) ferromagnets, (ii) ferrimagnets, (iii) antiferromagnets, (iv) weak ferromagnets (canted antiferromagnets), (v) metamagnets, (vi) spin glasses, etc.

The technologically useful switching between magnetic states leading to multifunction behavior is rare and has been limited to paramagnetic spin-crossover, photoinduced magnetic, and metamagnetic materials. Spin crossover materials switch from a low spin to a high spin paramagnetic state because of an external stimuli, which is typically thermal. However, spin crossover transitions can also be accomplished via light (LIESST) or pressure.[4] Magnetically ordered materials can be altered via light[5] or pressure[6,7] to form a paramagnetic or differently ordered state. Metamagnets are well-studied materials that exhibit a transition from an antiferromagnetic state to a high-moment ferromagnetic-like state with the application of an applied field.[8]

Recently, $Mn^{II}(TCNE)[C_4(CN)_8]_{1/2}\cdot zCH_2Cl_2$[9] was reported to have an antiferromagnetic ground state.[10] It has corrugated layers of Mn^{II} ions bonded to four $S = {}^1/_2$ μ_4-$[TCNE]^{\bullet-}$, and these layers are bridged by the diamagnetic ($S = 0$) μ_4-$[C_4(CN)_8]^{2-}$ dimer (Figure 1). $Mn(TCNE)[C_4(CN)_8]_{1/2}$ is attributed to having direct, antiferromagnetic exchange coupling between the $S = {}^5/_2$ Mn^{II} and the $S = {}^1/_2$ μ_4-$[TCNE]^{\bullet-}$ spin sites, leading to 2D ferrimagnetic layers. The ferrimagnetic layers antiferromagnetically couple via five-atom, conjugated $-N{\equiv}C-C-C{\equiv}N-$ superexchange pathways, leading to a bulk antiferromagnet.[10]

$Mn^{II}(TCNE)[C_4(CN)_8]_{1/2}\cdot zCH_2Cl_2$ has an antiferromagnetic ground state at ambient pressure.[10] On the basis of Fisher's "specific heat", $d\chi T/dT$ [χ = molar magnetic susceptibility,[11] and the temperature, T, at which the maximum in the 5 Oe zero-field-cooled (ZFC) and coincident field-cooled (FC) $M(T)$ (M = molar magnetization) data occur], T_c is 69 K.

Here, we report that under an applied hydrostatic pressure $Mn(TCNE)[C_4(CN)_8]_{1/2}$ is reversibly transformed from having an antiferromagnetic ground state to having an induced

Received: July 9, 2012
Published: August 31, 2012

   dx.doi.org/10.1021/ic3014865 | Inorg. Chem. 2012, 51, 9978−9982

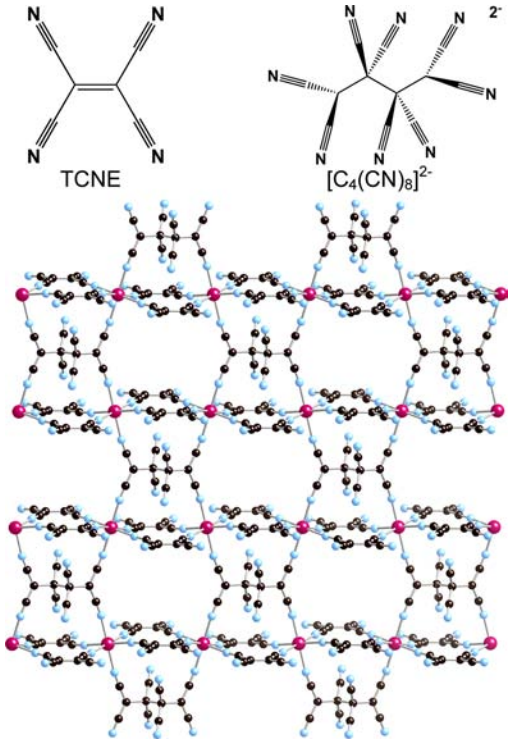

Figure 1. Extended network structure of $Mn^{II}(TCNE)[C_4(CN)_8]_{1/2}\cdot zCH_2Cl_2$[9] possessing μ_4-$[TCNE]^{\bullet-}$ in two dimensions, in which these layers are bridged by μ_4-$[C_4(CN)_8]^{2-}$ to form an extended 3D lattice. Color code: Mn is maroon, N is blue, and C is black. The disordered CH_2Cl_2 solvent fills the channels.

ferrimagnet state with a much enhanced T_c and not a higher T_c antiferromagnet. Pressure has been used in the past to increase {e.g., $[Fe(C_5Me_5)_2][TCNE]$[12] and β-4′-cyanotetrafluorophenyldithiadiazolyl][13]} or decrease {e.g., 4-nitrophenylnitronyl nitroxide[14] $[TDAE]^+[C_{60}]^-$ [TDAE = tetrakis(dimethylamino)ethane][15]} T_c for several organic-based magnets. In addition to lowering the T_c value, a transition from a ferromagnetic to an induced antiferromagnetic state was reported for 4-nitrophenylnitronyl nitroxide.[7] Also, some traditional antiferromagnets, e.g., $NMe_4[Mn^{II}Cl_3]$[16] and $Cs[Mn^{III}F_4]$,[17] respectively, have a decreased or increased T_c with applied pressure.

EXPERIMENTAL SECTION

$Mn^{II}(TCNE)[C_4(CN)_8]_{1/2}\cdot zCH_2Cl_2$ was prepared as previously reported.[10] For hydrostatic pressure studies, ∼1 mg was loaded into a Teflon sample holder in a drybox (<1 ppm O_2). In addition to the sample, ∼3 mg of a cylindrical 1.0-mm diameter piece of lead (Alfa Aesar, 99.998%) and ∼2 mg of decalin were added to the Teflon holder. Decalin was used as a hydrostatic pressure fluid, and lead was used as an internal pressure standard. At each pressure, the superconducting T_c of lead was used as a calibration of the applied pressure because the linear T_c dependence on the pressure of lead is known.[18] The Teflon holder was loaded into a Kyowa Seisakusho Be−Cu hydrostatic pressure cell with zirconia pistons and O-rings. The pressure was applied by using a Kyowa Seisakusho CR-PSC-KY05-1 pressure cell apparatus (≤16 kbar), with a WG-KY03-3 pressure sensor. An Aikoh Engineering model 0218B digital sensor was used as a digital readout for the pressure.

All magnetic measurements were performed using a Quantum Design MPMS-5XL 5T SQUID magnetometer equipped with a reciprocating sample measurement system, low-field option, and continuous low-temperature control with enhanced thermometry features. The temperature dependence of the magnetization was obtained upon cooling in zero applied field, and data were collected upon warming. The remnant magnetization was measured in zero applied field upon warming after cooling below T_c in an applied field of 5 Oe. The isothermal field-dependent magnetization was obtained by cooling to 8 K in zero applied field, and data were collected as the field was varied. The samples were placed separately inside a gelatin capsule for ambient-pressure measurements. The gelatin capsule ambient pressure data were compared to the pressure cell ambient pressure data, and a minor adjustment was made to correct for the diamagnetic contribution from the pressure cell.

RESULTS AND DISCUSSION

The ZFC, $M_{ZFC}(T,P)$, and 5 Oe FC, $M_{FC}(T,P)$, magnetizations up to 12.6 kbar applied hydrostatic pressure were measured between 8 and 200 K for $Mn^{II}(TCNE)[C_4(CN)_8]_{1/2}\cdot zCH_2Cl_2$ (Figure 2a). The ambient pressure $M_{ZFC}(T)$ and $M_{FC}(T)$ are coincident, lack a bifurcation temperature, T_b, and thus also lack any magnetic irreversibility, and have a broad maxima at 68 K, in accordance with the aforementioned ambient data characterizing the material as an antiferromagnet. Upon application of 0.95 kbar, $M_{ZFC}(T,P)$ and $M_{FC}(T,P)$ no longer are coincident and exhibit a T_b value of 30 K. T_b increases with increasing pressure and is 105 K at the maximum pressure studied (12.6 kbar; Figure 2b). Above ∼1 kbar, $T_b(P)$ increases linearly with the applied pressure at a rate of 6.6 K/kbar, and the FC magnetization increases by 3 orders of magnitude at low temperature in the ferrimagnetic state with increasing pressure.

To further investigate the lower pressure magnetic response, additional lower pressure data were taken on an independent, second sample that was quite similar. Antiferromagnetic behavior was additionally observed at 0.35 kbar, and ferrimagnetic behavior was observed at 0.65 kbar (Figure 2b). Hence, the transition from the antiferromagnetic ground state to a high-moment, ferrimagnetic excited state occurs between 0.35 and 0.65 kbar.

Below 0.65 kbar, $Mn^{II}(TCNE)[C_4(CN)_8]_{1/2}$ magnetically orders at ∼66 K, and again neither a coercive field, bifurcation temperature, nor remnant magnetization is observed, in accordance with the antiferromagnetic ground state. Hence, $Mn^{II}(TCNE)[C_4(CN)_8]_{1/2}$ is an antiferromagnet below 0.50 ± 0.15 kbar with a relatively independent T_c of 66 K.

The remnant magnetization, $M_r(T,P)$, up to 12.6 kbar was also measured between 8 and 200 K (Figure 2c), and similar data are observed for the aforementioned second, independent sample. At ambient pressure, $M_r(T,P)$ exhibits atypical behavior in that at low temperature it is negative and reaches a maximum value of only 0.41 emu Oe^{-1} mol^{-1} at ∼62 K, indicative of its bulk antiferromagnetic properties, as previously reported.[10] $M_r(T,P)$ becomes significant, increases with increasing pressure above 0.50 ± 0.15 kbar, and upon extrapolation of the 0.35 kbar $M_r(T,P)$ to zero gives a T_c of ∼20 K. T_c is similar to T_b, increases linearly with increasing pressure (6.2 K/kbar), and is ∼97 K at 12.6 kbar (Figure 2b), and the magnetization increases by 3 orders of magnitude at low temperature in the ferrimagnetic state with increasing pressure.

The hysteresis, $M(H,P)$, was measured at 8 K up to 12.6 kbar for $Mn(TCNE)[C_4(CN)_8]_{1/2}$ (Figure 3) and likewise is similar to that observed for the second, independent sample. At ambient pressure, $Mn(TCNE)[C_4(CN)_8]_{1/2}$ does not exhibit a hysteresis and has a saturation magnetization, M_s, of 20400 emu Oe^{-1} mol^{-1}. This value is less than the expected saturation magnetization of 22340 emu Oe^{-1} mol^{-1} for antiferromagnetic coupling. $M(H,P)$ significantly changes shape upon the

dx.doi.org/10.1021/ic3014865 | Inorg. Chem. 2012, 51, 9978−9982

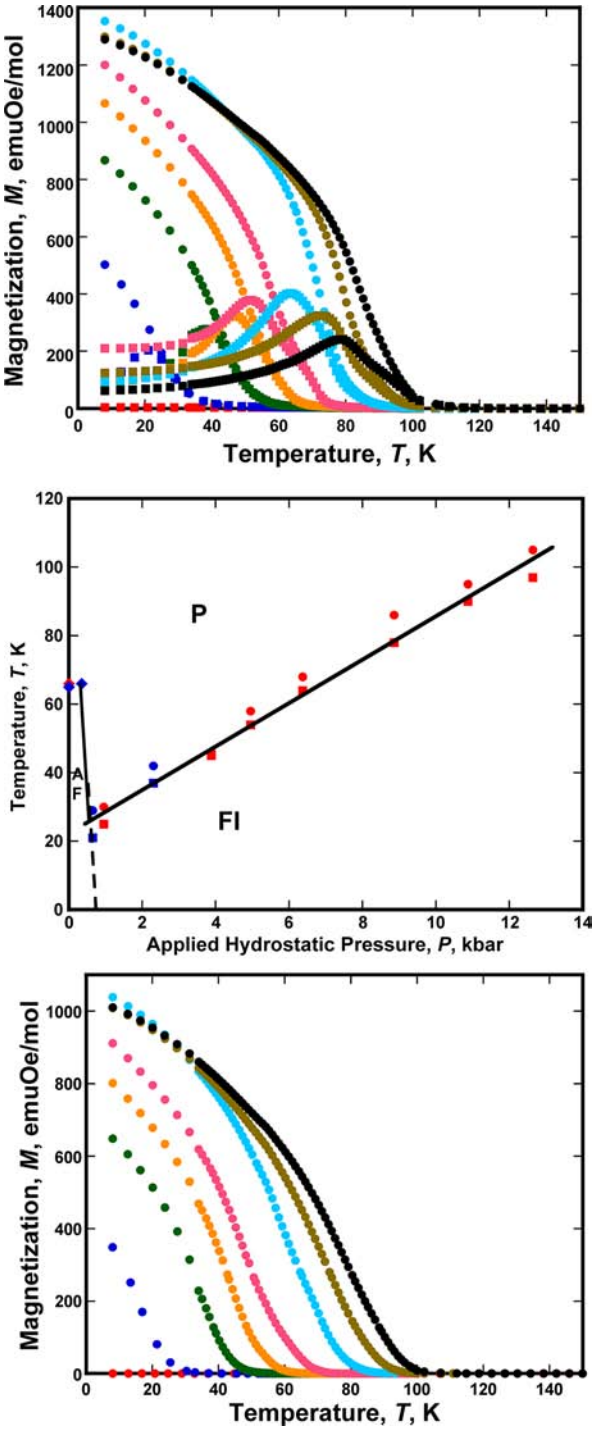

Figure 2. (top) $M_{ZFC}(T,P)$ and $M_{FC}(T,P)$ for Mn(TCNE)-$[C_4(CN)_8]_{1/2}$: ambient-pressure ZFC (red ■), FC (red ●); 0.95 ZFC (blue ■), FC (blue ●); 3.88 ZFC (green ■), FC (green ●); 4.95 ZFC (orange ■), FC (orange ●); 6.37 ZFC (pink ■), FC (pink ●); 8.86 ZFC (light-blue ■), FC (light-blue ●); 10.8 ZFC (brown ■), FC (brown ●); 12.6 kbar ZFC (black ■), FC (black ●). (middle) $T_c(P)$ (■) from $M_r(T,P)$ and $T_b(P)$ (●) and $T_c(P)$ (antiferromagnetic) (◆) from $M_{ZFC}(T,P)$ and $M_{FC}(T,P)$ for ferrimagnetic $Mn^{II}(TCNE)[C_4(CN)_8]_{1/2}$ [samples 1 (red) and 2 (blue)]. AF = antiferromagnetic; P = paramagnetic; FI = ferrimagnetic. (bottom) $M_r(T,P)$ for Mn(TCNE)$[C_4(CN)_8]_{1/2}$: ambient-pressure (red ●), 0.95 (blue ●), 3.88 (green ●), 4.95 (orange ●), 6.37 (pink ●), 8.86 (light-blue ●), 10.8 (brown ●), and 12.6 kbar (black ●).

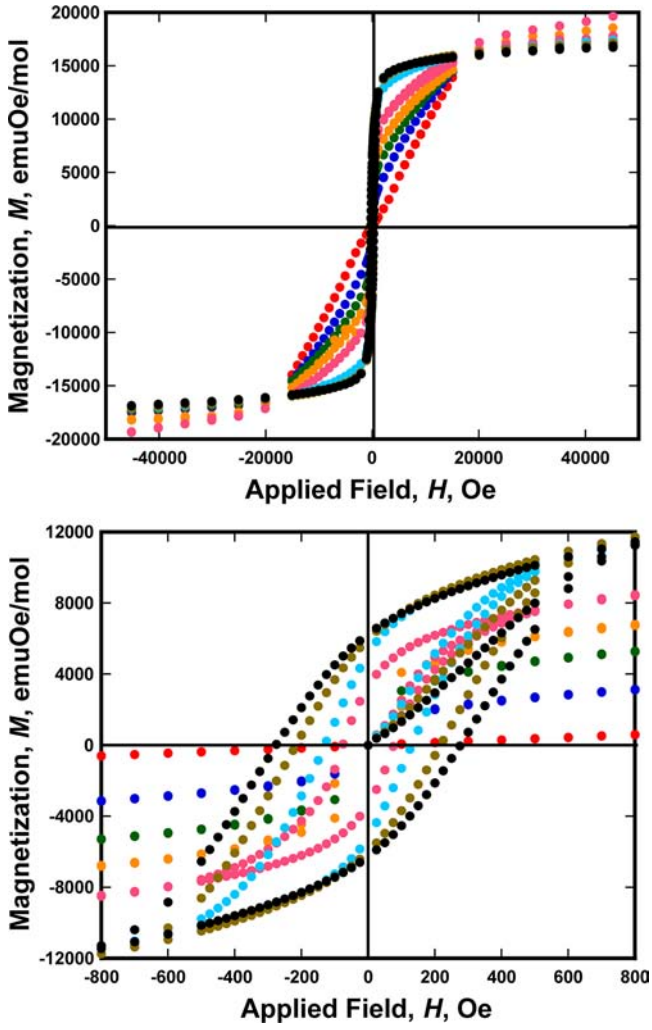

Figure 3. $M(H,P)$ (top) and zoom-in (bottom) showing hysteresis (bottom) for $Mn^{II}(TCNE)[C_4(CN)_8]_{1/2}$: ambient pressure (red ●), 0.95 (blue ●), 3.88 (green ●), 4.95 (orange ●), 6.37 (pink ●), 8.86 (light-blue ●), 10.8 (brown ●), and 12.6 kbar (black ●).

application of pressure, leading to an induced hysteretic behavior. Below 3.88 kbar, $M(H,P)$ is similar to the ambient-pressure $M(H,P)$ data because there is neither a coercive field, H_{cr}, nor a remnant magnetization, M_r, and M_s exhibits a slight decrease. At 3.88 kbar, $M(H,P)$ exhibits a coercive field and remnant magnetization, and H_{cr} and M_r continually increase with increasing pressure (Figure 4) and reach 280 Oe and 6200 emu Oe^{-1} mol^{-1}, respectively, at 12.6 kbar.

The application of pressure on $Mn^{II}(TCNE)[C_4(CN)_8]_{1/2}$ is qualitatively reversible because, upon release of the applied pressure back to ambient, the induced ferrimagnetic behavior disappears and the original antiferromagnetic properties are observed; i.e., there is no bifurcation temperature in the $M_{ZFC}(T,P)$ and $M_{FC}(T,P)$ data (Figure S1a in the Supporting Information), the magnitude of $M_r(T,P)$ is small for the entire temperature range (Figure S1b in the Supporting Information), and the hysteretic behavior that is induced with pressure is no longer observed (Figure S1c in the Supporting Information). Although the original antiferromagnetic ground state is observed, the values and shapes of $M_{ZFC}(T,P)$, $M_{FC}(T,P)$, $M_r(T,P)$, and $M(H,P)$ change slightly, and this is attributed to the possible formation of defects.

dx.doi.org/10.1021/ic3014865 | Inorg. Chem. 2012, 51, 9978–9982

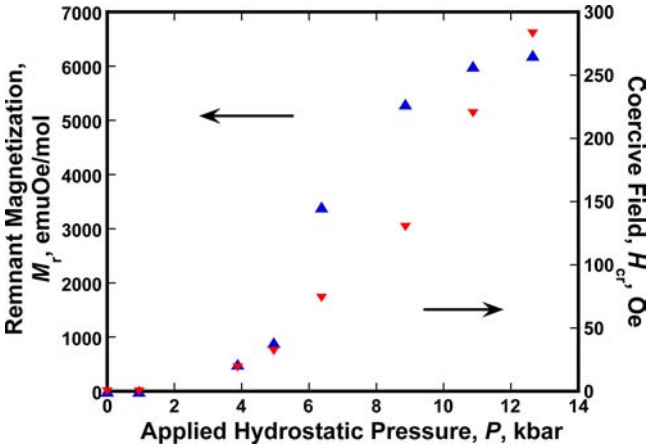

Figure 4. $H_{cr}(P)$ (red ▼) and $M_r(P)$ (blue ▲) for ferrimagnetic $Mn^{II}(TCNE)[C_4(CN)_8]_{1/2}$.

$Mn^{II}(TCNE)[C_4(CN)_8]_{1/2}$ undergoes a magnetic transition from an antiferromagnetic to a high-moment state between 0.50 ± 0.15 kbar. This suggests that only a small change in the structure occurs in this pressure regime. At higher pressure, however, a transition to a high-moment ferrimagnetic state occurs. This transition is akin to a metamagnetic, but it is pressure, not temperature, induced.[8] The dramatic change in the magnitude and shape of the $M_{ZFC}(T,P)$ and $M_{FC}(T,P)$ data suggests that the dominant interlayer interactions are altered with the application of pressure going from an antiferromagnet to a ferrimagnet. This is in agreement with the remnant data in which the ambient-pressure measurement shows little or no remnant magnetization; however, with the application of pressure, it shows significant remnant magnetization typical of ferrimagnets. The $M(H,P)$ data are also in accordance with the lack of hysteresis at ambient pressure and, upon the application of pressure, exhibit hysteresis indicative of ferrimagnetic ordering.

This suggests a significant increase in the coupling between the 2D ferrimagnetic layers that may be attributed to structural changes, such as slipping, between the layers that lead to canting of the moments. This would produce an incomplete cancellation of moments between the layers, leading to a transition from an antiferromagnet to a canted antiferromagnet (weak ferromagnet), and increasing the pressure would increase the canting and coupling, ultimately enhancing T_c.

It is also possible that the diamagnetic bridging μ_4-$[C_4(CN)_8]^{2-}$ forms some $S = {}^1/_2$ *cis*-μ-$[TCNE]^{\bullet-}$ under pressure and thus (i) provides a pathway for interchain coupling that will lead to ferrimagnetic behavior and (ii) strongly enhances the interchain coupling increasing T_c, as are observed for $Mn(TCNE)_{3/2}I_{3/2}$.[9] The formation of $[TCNE]^{\bullet-}$ increases the number of the $S = {}^1/_2$ *cis*-μ-$[TCNE]^{\bullet-}$ antiferromagnetically coupled to the $S = {}^5/_2$ Mn^{II} site, decreasing the saturation magnetization, as is observed.

CONCLUSION

$M(T,H,P)$ of $Mn(TCNE)[C_4(CN)_8]_{1/2}$ reveals a reversible pressure-induced magnetic transition from antiferromagnet to ferrimagnet. In addition, an enhancement of T_c up to 97 K with applied pressure is observed for the ferrimagnetic state. This is attributed to structural changes that lead to either the formation of $S = {}^1/_2$ *cis*-μ-$[TCNE]^{\bullet-}$ between the layers or spin canting leading to incomplete cancellation of moments between the layers. The phase diagram showing the coexistence between the paramagnetic (P), antiferromagnetic (AF), and ferrimagnetic (FI) phases is depicted in Figure 2b.

Pressure-induced magnetic transitions have been previously reported for other magnetic materials including antiferromagnetic to ferri- or ferromagnetic,[19−21] as observed for $Mn^{II}(TCNE)[C_4(CN)_8]_{1/2}$, antiferromagnetic to paramagnetic,[22] and ferromagnetic to antiferromagnetic,[7,23−25] as well as between ferrimagnetic states.[6] $Fe^{II}(TCNE)[C_4(CN)_8]_{1/2}$ also undergoes a transition from an antiferromagnet state to a ferrimagnetic state with applied pressure but additionally undergoes an applied magnetic field metamagnetic transition at ambient pressure and is under study. These piezomagnetic transitions suggest applications in transducers, sensors, and actuators.

ASSOCIATED CONTENT

Supporting Information

$M_{ZFC}(T,P)$, $M_{FC}(T,P)$, and $M_r(T,P)$ at ambient pressure and after pressure release. This material is available free of charge via the Internet at http://pubs.acs.org.

AUTHOR INFORMATION

Corresponding Author

*E-mail: jsmiller@chem.utah.edu.

Notes

The authors declare no competing financial interest.

†Deceased May 7, 2012; http://www.meaningfulfunerals.net/fh/obituaries/obituary.cfm?o_id=1476970&fh_id=13348.

ACKNOWLEDGMENTS

We appreciate continued support by the Department of Energy Division of Material Science (Grant DE-FG03-93ER45504).

REFERENCES

(1) Miller, J. S.; Calabrese, J. C.; Epstein, A. J.; Bigelow, R. W.; Zhang, J. H.; Reiff, W. M. *J. Chem. Soc., Chem. Commun.* **1986**, 1026.
(2) Manriquez, J. M.; Yee, G. T.; McLean, R. S.; Epstein, A. J.; Miller, J. S. *Science* **1991**, *252*, 141.
(3) Miller, J. S. *Polyhedron* **2009**, *28*, 1596.
(4) *Spin Crossover in Transition Metal Compounds I*; Gütlich, P., Goodwin, H. A., Eds.; Topics in Current Chemistry; Springer: New York, 2004; Vol. *233*.
(5) Varret, F.; Nogues, M.; Goujon, A. In *Magnetism: Molecules to Materials*; Miller, J. S., Drillon, M., Eds.; Wiley-VCH: New York, 2000; Vol. *1*, p 257.
(6) Coronado, E.; Giménez-López, M. C.; Korzeniak, T.; Levchenko, G.; Romero, F. M.; Segura, A.; García-Baonza, V.; Cezar, J. C.; de Groot, F. M. F.; Milner, A.; Paz-Pasternak, M. *J. Am. Chem. Soc.* **2008**, *130*, 15519.
(7) Takeda, T.; Mito, M. In *Carbon-based magnetism*; Makarova, T., Palacio, F., Eds.; Elsevier: Amsterdam, The Netherlands, 2006; pp 131−158.
(8) Stryjewski, E.; Giordano, N. *Adv. Phys.* **1977**, *26*, 487.
(9) Stone, K. H.; Stephens, P. W.; McConnell, A. C.; Shurdha, E.; Pokhodnya, K. I.; Miller, J. S. *Adv. Mater.* **2010**, *22*, 2514.
(10) McConnell, A. C.; Shurdha, E.; Bell, J. D.; Miller, J. S. *J. Phys. Chem. C* **2012**, *116*, 0000 DOI: 10.1021/jp302765d.
(11) Fisher, M. E. *Philos. Mag.* **1962**, *7*, 1731.
(12) Huang, Z. J.; Cheng, F.; Ren, Y. T.; Xue, Y. Y.; Chu, C. W.; Miller, J. S. *J. Appl. Phys.* **1993**, *73*, 6563.
(13) Mito, M.; Takawae, T.; Takeda, T.; Takagi, S.; Matsushita, Y.; Deguchi, H.; Rawson, J. M.; Palacio, F. *Polyhedron* **2001**, *20*, 1509.
(14) Takeda, K.; Konishi, K.; Tamura, T.; Kinoshita, M. *Phys. Rev. B* **1996**, *53*, 3374.

(15) Thompson, J. D.; Sparn, G.; Diederich, F.; Gruner, G.; Holczer, K.; Kaner, R. B.; Whetten, R. L.; Allemand, P. M.; Li, Q.; Wudl, F. *Mater. Res. Soc. Symp.* **1992**, *247*, 315.
(16) Tancharakorn, S.; Fabbiani, P. A.; Allan, D. R.; Kamenev, K. V.; Robertson, N. *J. Am. Chem. Soc.* **2006**, *128*, 9205.
(17) Ishizuka, M.; Henmi, S.; Endo, S.; Morón, M. C.; Palacio, F. *J. Magn. Magn. Mater.* **1999**, *196*−*7*, 440.
(18) Clark, M. J.; Smith, T. F. *J. Low Temp. Phys.* **1978**, *32*, 495.
(19) Umeo, K.; Yamane, H.; Kubo, H.; Muro, Y.; Takabatake, T. *J. Phys. Conf. Ser.* **2010**, *200*, 012215.
(20) Egan, L.; Kamenev, K.; Papanikolaou, D.; Takabayashi, Y.; Margadonna, S. *J. Am. Chem. Soc.* **2006**, *128*, 6034.
(21) Yamamoto, T.; Tassel, C.; Kobayashi, Y.; Kawakami, T.; Okada, T.; Yagi, T.; Yoshida, H.; Kamatani, T.; Watanabe, Y.; Kikegawa, T.; Takano, M.; Yoshimura, K.; Kageyama, H. *J. Am. Chem. Soc.* **2011**, *133*, 6036.
(22) Tajiri, T.; Matsumoto, S.; Deguchi, H.; Mito, M.; Takagi, S.; Moriyoshi, C.; Itoh, K.; Koyama, K. *J. Magn. Magn. Mater.* **2007**, *310*, e566.
(23) Yamada, A.; Matsubayashi, K.; Uwatoko, Y.; Kondo, K.; Katano, S.; Kosaka, M. *Solid State Commun.* **2010**, *150*, 725.
(24) Mitrofanov, V. Y.; Nikiforov, A. E.; Shashkin, S. Y. *Solid State Commun.* **1997**, *104*, 499.
(25) Okada, H.; Koyama, K.; Miura, S.; Yamada, M.; Goto, T.; Makihara, Y.; Fujii, K.; Watanabe, K. *J. Phys. Soc. Jpn.* **2004**, *73*, 1982.